

Internal Stress in the Porous Anodic Alumina/Aluminum System

^{1,*} Valentina YAKOVITSEVA, ¹ Vladimir SHULGOV
and ¹ Dzmitry SHIMANOVICH

¹ Belarusian State University of Informatics and Radioelectronics, 6 Brovka, Minsk, 220013, Belarus

¹ Tel.: +375172938850

* E-mail: yakovitseva@yahoo.com

Received: 20 November 2020 / Accepted: 9 January 2021 / Published: 29 January 2021

Abstract: The internal stresses of the aluminum films deposited at various substrate temperatures and evaporation rates are studied. It is shown that tensile stresses are present in the aluminum film. The tensile stresses values are equal to $(1.0-3.5) \cdot 10^7$ N/m² to be comparable with the aluminum yield point ($2.3 \cdot 10^7$ N/m²). Theoretical and experimental studies of deformation and stress at the porous aluminum oxide-aluminum interface are discussed. It is shown that the internal stresses in the growing porous oxide are always compressive stresses and practically do not depend on the internal stresses in the initial aluminum film. The last testifies the fact of reaching the aluminum yield point at the oxide formation.

Keywords: Aluminum, Anodic alumina, Two-layer system, Internal stress, Deformation.

1. Introduction

In recent years, there is an intensive development of sensor technology that reaches a new level of sensitivity. Electrochemical, acoustic, optical sensors and biosensors are developed. Among the optical sensors, it should be noted the devices on the surface plasmon resonance (SPR), reflectometric spectroscopy sensors, waveguide sensors, including waveguide sensors on a metal underlayer (WSMP). WSMP which is a thin film structure consisted of a waveguide layer of porous anodic aluminum oxide on the aluminum sublayer is of particular interest. Technology of coatings based on anodic alumina for sensor applications (SPR- sensors and WSMP) includes the following stages: the vacuum deposition of aluminum films on the dielectric substrate; the one-step anodic oxidation for the formation of the alumina film and a translucent aluminum film; the chemical etching for widening of pores with controlled optical

parameters of nanostructured coatings. So, control of mechanical stress of the film on the basis of which the device is formed is very important for designing devices with required parameters [1-3].

Recently it is well-known that stress takes place in the system oxide-metal both in the oxide growth process and in the stable state. Beginning from Pilling and Bedworth [4], who were the first to pay attention to the significance of the volumetric ratio between metal and its oxide (Pilling-Bedworth ratio), a lot of investigators have attempted to detect, measure and explain stresses in the oxide-metal system resulting from the difference in the specific volumes of oxide and metal. However, results of theoretical and experimental investigations of the internal stresses that appear in oxide ceramic coatings formed by plasma-electrolytic oxidation (PEO) on aluminum surfaces were reported to be always much lower than calculated by the coefficients of the volume growth [5]. It turned out that the coefficient of the oxide volume increase is

not the only factor determining a stress level and that a mechanism of the metal conversion into oxide is realized to provide minimum stress. In this connection a key role of the motion of anions and cations in the process of the oxide growth was pointed out. Recently this concept provides the basis on which the internal stresses in the oxide-metal system can be studied. In accordance with this concept, the stress value depends on a number of transferred anions and cations and is a maximum in the case of the 100 % anion transfer, resulting in a compressive stress in oxide and a tensile stress in metal. Depending on the stress value during the oxide growth, metal can undergo elastic or even plastic deformation. In this case the dislocation motion, accumulation and transition through the metal-oxide interface are inevitable. The dislocation presence to a greater or lesser extent when they act as vacancy sinks can change the oxidation kinetics because the vacancy diffusion along the dislocation is facilitated.

Thus, a pronounced stress effect on the oxidation process is obvious. So, it is of theoretical and practical importance to know the state of the two-layer oxide-metal system as a whole and the effect of the formation conditions of both the aluminum film and porous oxide on the stress level.

2. Experimental

Electron-beam evaporation was used for the aluminum deposition on the 165 μm thick rectangular glass strips in the length-to-width ratio of 10:1 to measure stresses by the console method as the simplest and easy-to-use method for the vacuum evaporated films. The stress σ was calculated by the Stoney's formula:

$$\sigma = \frac{Ed^2x}{3l^2h(1-\mu)}, \quad (1)$$

where E is the modulus of elasticity (Young modulus) for the substrate; d is the substrate thickness; x is the flexure of the free end; l is a substrate length; h is the thickness of the evaporated film; μ is the Poisson's ratio.

The modulus of elasticity for the substrate was measured by hanging of a plummet to the console end and determining of the glass flexure. This was calculated by the formula:

$$E = \frac{4Gl^3}{wd^3x}, \quad (2)$$

where G is the plummet weight, and w is the substrate width. Young modulus was equal to $5 \cdot 10^{10}$ N/m².

The aluminum evaporation was made at various substrate temperatures and deposition rates. The flexure values x were measured at the room

temperature when the samples were taken out of the vacuum chamber.

The internal stress in the two-layer "porous alumina–aluminum" system was studied theoretically and experimentally during the aluminum anodization. To this end, an experimental assembly was made allowing a deflection of the glass console with the deposited aluminum film from the initial position to be measured directly the porous anodization process. A design of the measurement unit of the assembly is shown in Fig. 1.

A sample of a squared shape is cramped in a special hermetic holder where a voltage is supplied to the aluminum film to be anodized. A negative potential is supplied to the cathode. The sample is entirely immersed into the electrolyte. A microscope ocular is provided with a scale. The end surface of the sample is aligned with the scale divisions in the microscope focus. During the anodization the sample end surface image shifts and a value of this shift is measured with the scale. To exclude the influence of electrostatic forces, a shift reading is made after the anodization voltage cut off.

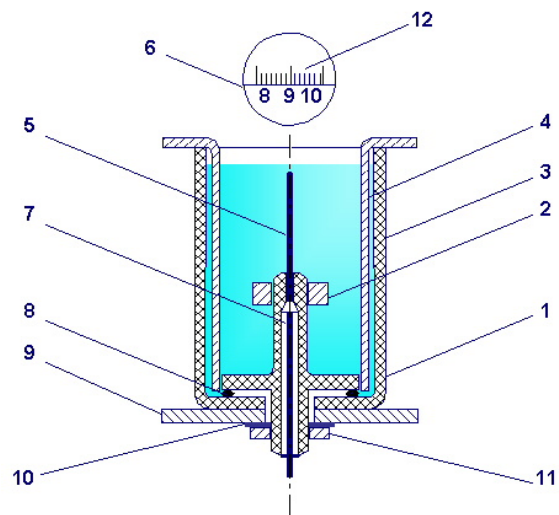


Fig. 1. A design of the basic unit (cell) of the experimental assembly: (1) Holder; (2) Special screw; (3) Cell; (4) Cylindrical cathode; (5) Sample; (6) Microscope ocular; (7) Anode; (8) Rubber gasket; (9) Stage; (10) Washer; (11) Screw; (12) The end surface of the sample.

With this assembly the console shift values from the initial position depending on the porous oxide thicknesses, current densities, and voltages were read.

3. Results and Discussion

3.1. Internal Stress in the Aluminum Films

Fig. 1 – Fig. 2 show dependences of the internal stresses calculated by the Eq. (1) on the thickness of the aluminum films deposited at various substrate temperatures and evaporation rates.

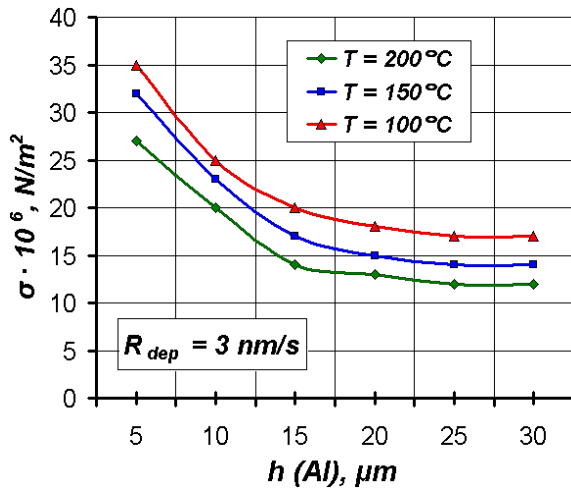


Fig. 2. Dependence of the internal stresses on the thickness of the aluminum films at various substrate temperatures.

Referring to Fig. 1, in the aluminum films the internal stresses are reduced with the increase in the film thickness and the substrate temperature. The glass substrate flexes towards the deposited film. This is indicative of the tensile stress presence in the aluminum film. In contrast to thin films, in more than 1 μm thick aluminum films the tensile stresses are reduced when the deposition rate increases, as shown in Fig. 3.

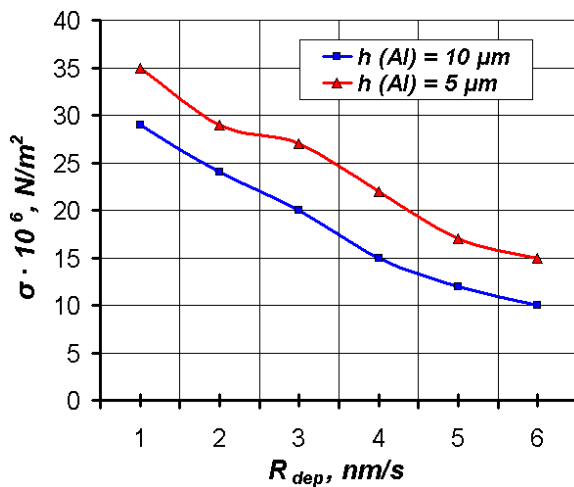


Fig. 3. Dependence of the internal stresses on the deposition rate of the aluminum films.

The tensile stresses values are equal to $(1.0-3.5) \cdot 10^7$ N/m² to be comparable with the aluminum yield point ($2.3 \cdot 10^7$ N/m²).

It is clear that stresses measured are characteristic of residual stresses including thermal stresses resulted from the difference in the linear expansion coefficients of aluminum and the substrate material. Thermal stresses are calculated by the formula:

$$\sigma_T = \Delta d \cdot \Delta T \cdot E / (1 - \mu), \quad (3)$$

where Δd is the difference in the linear expansion coefficients of aluminum and glass; ΔT is the difference between the condensation point and the room temperature; μ is a Poisson's ratio.

For aluminum $\mu = 0.348$ and $\sigma_T = (2-3) \cdot 10^8$ N/m² to be 10 times higher than residual stresses. This is evidence of high ability of the aluminum films to a stress relaxation by means of a plastic deformation.

Thus, the aluminum films are plastically deformed. So, they have a developed dislocation arrangement up to the structure typical of the afterflow stage when a splitting of the initial aluminum grains is possible due to the net of dislocation clusters. However, to all appearance such the structure is not characteristic of the whole thickness of the aluminum film. The reduction of the internal stresses in the film-substrate system with the aluminum thickness and the deposition rate, as discussed above, testifies that in this case not a two-layer system but at the least a three-layer one consisting of the substrate, a transition plastically deformed aluminum layer, and an outer elastically stressed aluminum layer should be considered. Then the stress reduction with the film thickness can be explained by the expansion of the transition layer. With thin aluminum films, the aluminum yield point increases almost by the order and therefore the relaxation of the stresses is difficult [5].

3.2. Deformation and Stress at the Porous Alumina-aluminum Interface

Based on the well-known fact about the sphericity of the interface "porous alumina cell/aluminum", we can ignore the influence of the free surface and assume that the deformation in the oxide-metal system will be approximately the same as in an infinite matrix (metal) with spherical inclusion (oxide). For this model, a solution of the known Eshelby task of an ellipsoidal inclusion in an array [7] may be used.

Let the inclusion is subjected to a transformation from which its relative volume increased by e^T as compared with the position outside of the matrix. Then, dilation e^T is equal to the sum of relative deformations e^T_{xx} , e^T_{yy} , and e^T_{zz} of the inclusion along the corresponding axes. If the elastic modulus of the matrix is equal to the elastic modulus of the inclusion, cubic strain e^0 of the array is defined by the following expression:

$$e^0 = \alpha e^T = \frac{1}{3} \cdot \frac{1+\nu}{1-\nu} e^T, \quad (4)$$

where ν is a Poisson's ratio.

The deformation e^I of the inclusion in the matrix is equal to:

$$e^I = e^T - e^c \quad (5)$$

If the transformation changes elastic modulus of the inclusion, this change may be taken into account by entering a new deformation e^{-T} free of stress. For uniform case, this strain e^{-T} correlates with e^T by the following expression:

$$e^{-T} = e^T \left[\frac{\chi}{\chi^*} + \alpha \left(1 - \frac{\chi}{\chi^*} \right) \right]^{-1}, \quad (6)$$

where χ and χ^* are compression moduli of the matrix and the inclusion correspondingly.

Evaluate the matrix deformation as applied to the alumina/aluminum system. Free dilation, which corresponds to an increase in the specific volume of the oxide (inclusion) by 1.5 times compared to the metal (matrix), is equal to 0.5. We set $\nu = \nu^* = 1/3$; modulus of elasticity for aluminum $E = 6.6 \cdot 10^{10}$ N/m²; modulus of elasticity for alumina $E^* = 2.7 \cdot 10^{11}$ N/m². In this case $\chi/\chi^* \approx E/E^* = 1/4$, and by formula (6) we find that $e^{-T} = 4/3e^T$. That is, greater inclusion rigidity results in an increase of 1/3 in e^T as compared with the case of equal moduli. The cubic deformation of the matrix determined by Formula (4) is equal to 0.355. A linear deformation comprises 1/3 of the cubic one and is equal to 0.1185.

The solution of the Eshelby task and the evaluation based on this solution are true in the elastic deformation range. It is obvious that high-plastic aluminum cannot be deformed elastically almost by 12 %. Therefore, a range of plastically deformed metal is formed near alumina. Determine a size of this range in the same approximation where the alumina cell is imaginable as the spherical inclusion within the metal matrix. To calculate the range thickness, we use the task of plastic deformation of a sphere with a cavity loaded from the inside by pressure, which is known in the theory of plasticity. As applied to our task, the inclusion may be considered as only inducing stress in the matrix. Two things should be taken into account:

1) The matrix, in contrast to the spherical shell, has an infinite extent;

2) A pressure (stress) at the inclusion-matrix interface is unknown. It is possible to take proper account of the first factor by tending an outer radius to infinity in the solution for sphere. Then the radius of the plastic strain range C near the spherical inclusion is defined by the following expression:

$$C = \alpha \exp \left(\frac{p}{2\sigma_s} - \frac{1}{3} \right), \quad (7)$$

where α is the radius of the inclusion; p is the pressure at the interface; σ_s is the yield point of matrix material. For the purely elastic task, p can be defined by the deformation e^l inside the inclusion. The plastic range formation results in a considerable stress relaxation at the inclusion-matrix interface, and p may be defined indirectly from the geometrical sizes of this range. Taking the logarithm of the expression (7), we obtain:

$$p = \frac{2\sigma_s}{3} \left(1 + 3 \ln \frac{C}{\alpha} \right) \quad (8)$$

Thus, to find p we should know the ratio C/α . The last we can find using the following expression for the displacement in the plastic deformation range:

$$U_r = \frac{r\sigma_s}{E} \left[(1-\nu) \frac{C^3}{r^3} - \frac{2}{3}(1-2\nu) \left(1 + 3 \ln \frac{C}{\alpha} \right) \right] \quad (9)$$

Here r is the radial coordinate of set point in the spherical coordinate system. The inclusion broadening is provided by the displacement of matrix material; in this case the ratio $e^T = 3U_{r-\alpha}/\alpha$ takes place, using which and neglecting $\ln C/\alpha$ in comparison with $(C/\alpha)^3$ from (9) obtain the expression for the relative radius of the range:

$$\frac{C}{\alpha} = \left[\frac{e^T E}{3\sigma_s (1-\nu)} \right]^{1/3} \quad (10)$$

A numerical evaluation by the formula (10) yields the range size $C-\alpha \approx 3\alpha$. For the calculation $e^T = 0.4$ and $\nu = 0.33$ were assumed. A value of σ_s was taken high by 8 times of the yield point of bulk cold-rolled aluminum ($2.3 \cdot 10^7$ N/m²) since this precise value for aluminum films is not defined so far, but it is known that material strength in a thin-film form is 3 – 10 times higher than this of bulk samples. Stress at the alumina-aluminum interface calculated by Formula (8) is equal to about $3.5\sigma_s$, correlating with the inclusion linear deformation of 0.8 %. The calculation in the framework of the theory of elasticity gives the inclusion linear deformation of about 1.5 %, i.e. practically the plastic range formation equal to three radii of the porous alumina cell decreases a stress level about by half.

From an early stage, the deformation of aluminum is accompanied by its hardening. Define the radius C and the pressure p of the range taking into account linear strengthening of the matrix. Taking into consideration the features of our task, we obtain the expression for the pressure at the inclusion-matrix interface:

$$p = \frac{2}{3} \frac{\sigma_s}{(1+4\omega M)} \left[M(1+4\omega) \frac{C^3}{\alpha^3} + n \left(1 + 3 \ln \frac{C}{\alpha} \right) + (1-n+4\omega M) \ln \frac{1-n+4\omega M}{M(1+\omega M)} \right] \quad (11)$$

Here $\omega = \frac{1-2\nu}{2(1+\nu)}$; $M = \frac{2m\sigma_s(1+\nu)}{\sqrt{3}E}$; m and n are constants.

The expression (11) for ideal plasticity ($n=1, m=0$) grades into (7). For the displacement \bar{U}_r , taking into account the strengthening, we obtain the following expression:

$$\bar{U}_r = \frac{r\sigma_s}{E(1+4\omega M)} \left\{ \begin{array}{l} (1-\nu)\frac{C^3}{\alpha^3} - \frac{2}{3}(1-2\nu) \cdot \\ n\left(1+3\ln\frac{C}{a}\right) + \\ (1-n+4\omega M)\ln\frac{1-n+4\omega M}{M(1+4\omega M)} \end{array} \right\} \quad (12)$$

Comparing the expressions (12) and (11), it is evident that the strengthening manifests itself as an appearance of a common multiplier $(1-4\omega M)^{-1}$, coefficient n before the second summand and the third summand. Using the expression (12), an equation for defining C/a taking into account the strengthening of material may be composed.

For the numerical evaluation, m and n constants should be defined where m is a strengthening coefficient represented as a slope ratio of the linear range in the deformation curve of the second stage and n is a segment on the voltage ordinate axis. The deformation curves for polycrystalline aluminum at the room temperature have a cusp form and do not show the linear range of the second strengthening stage. If we approximate the parabolic deformation curves for the 99.999 % pure aluminum with linear functions, we obtain that $n \approx 1$, $m \approx 5$. It is noticeable that the deformation curves depend considerably on the metal graininess and in our case it should be guided by the curve for the large-grained sample because the cell size is less than the crystal size. The numerical evaluation of the strengthening effect on the plastic range radius shows that it slightly ($\sim 1\%$) decreases. This results from the small enough value of the aluminum strengthening coefficient. The evaluation of stress at the phase interface by (11) shows that it increases up to $p \sim 5.6\sigma_s$, i.e. by 40 % higher than obtained by (8).

Thus, the deformation calculation in the framework of the theory of elasticity disclosed that aluminum plastic deformation should occur at the alumina-aluminum interface. In this case the plastic deformation range is equal to about three radii of a barrier region of porous alumina. Integrally the porous alumina-aluminum interface should be presented by way of several characteristic ranges as shown in Fig. 4.

The range of elastically deformed aluminum transferring into the range of plastically deformed metal is located between initial aluminum and formed porous oxide. The width of the plastic deformation range is equal to three radii of the spherical base of the porous oxide cell. The relaxation of the internal stresses takes place in the plastic deformation range to be associated with the increase of the dislocation density and the formation of the dislocation net causing grain splitting. To all appearance, this explains independence of the porous oxide cell morphology on the initial structure of the aluminum film.

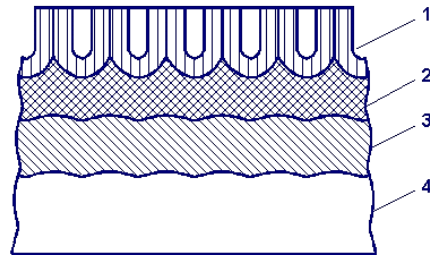


Fig. 4. The porous alumina-aluminum interface: (1) porous alumina; (2) a range of plastically deformed aluminum; (3) a range of elastically deformed aluminum; (4) aluminum.

To check the above calculations, the internal stresses in the “porous anodic alumina-aluminum” system were studied experimentally during the aluminum anodization. With the assembly described above the console shift values from the initial position depending on the porous oxide thicknesses, current densities, and voltages were read. These dependences are presented in Fig. 5 and Fig. 6. The σ – dependence on the oxide thickness was obtained at the anodization in 4% aqueous solution of the oxalic acid. The dependence shown in Fig. 6 was obtained at the anodization in various electrolytes.

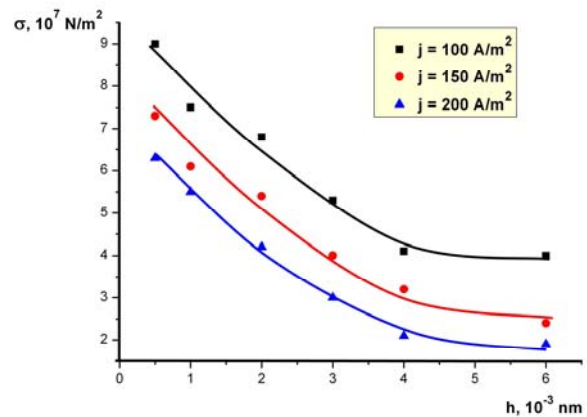


Fig. 5. Dependence of the internal stresses on the thickness of porous alumina.

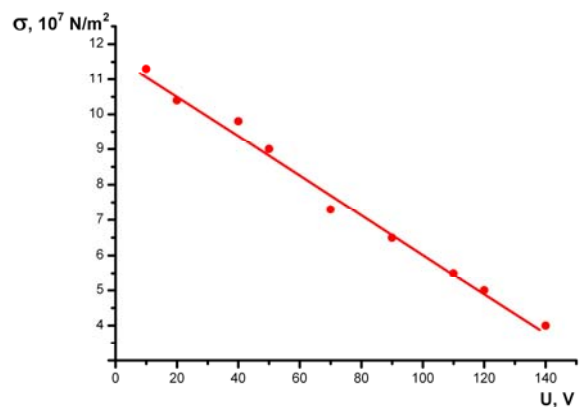


Fig. 6. Dependence of the internal stresses in alumina on the anodization voltage.

For anodization voltages up to 30 V the solutions of the sulfuric acid were used. The anodization with the voltage in the range from 30 V to 70 V was made in the oxalic acid solutions. When anodized with the voltage above 70 V, the aqueous solutions of the orthophosphoric acid were used. The solution concentrations were selected to provide the same anodization current density.

As seen from Fig. 5, the internal stresses in the porous oxide decrease with the oxide thickness increase and the current density rise. Referring to Fig. 6, the internal stresses decrease as well with the increase in the formation voltage. However, it is significant that the value of these stresses is comparable with the aluminum yield point for all cases while the above calculations show that the internal stresses at the oxide-metal interface can be few times above the yield point. It is well-known that at $\sigma > \sigma_s$ aluminum undergoes structural transformations characteristic of the afterflow stage, resulting in the internal stress relaxation up to the level $\sigma \approx \sigma_s$. Therefore, in the ideal case we should to have had a constant σ value close to σ_s irrespective of the parameters shown in Fig. 5. Obviously, the deviation from ideality is referred to the dependence of the relaxation level of the internal stresses on both the oxide layer thickness (Fig. 5) and the plastically deformed aluminum range width (Fig. 4).

The internal stresses in the growing porous oxide were found in these experiments to be always compressive stresses (the console flexes in the direction opposite to the oxide location) and are practically independent on the internal stresses in the initial aluminum film. The last once more testifies the fact of reaching the aluminum yield point at the oxide formation.

4. Conclusions

Thus, the analysis of the internal stresses in deposited aluminum layers has showed that internal stress in aluminum films decreases with increasing film thickness and substrate temperature. Tensile stresses are present in the aluminum film. At the same

time, in aluminum films with a thickness of more than 1.103 nm, the tensile stress decreases with an increase in the deposition rate.

Theoretical and experimental studies of deformation and stress at the porous aluminum oxide-aluminum interface have shown that the internal stresses in the growing porous oxide are always compressive stresses and practically do not depend on the internal stresses in the initial aluminum film.

The study may be applied to fabricate the nanoporous alumina coatings for different kinds of high-sensitive sensors.

References

- [1]. M. Pletea, W. Bruckner, H. Wendrock, R. Kaltofen, Stress evolution during and after sputter deposition of Cu thin films onto Si (100) substrates under various sputtering pressures, *Journal of Applied Physics*, Vol. 97, Issue 5, 2005, pp. 4908-4914.
- [2]. P. Coman, V. N. Juzevych, Internal mechanical stresses and the thermodynamic and adhesion parameters of the metal condensate – single-crystal silicon system, *Physics of the Solid State*, Vol. 54, Issue 7, 2012, pp. 1417-1424.
- [3]. B. W. Sheldon, K. H. A. Lau, A. Rajamani, Intrinsic stress, island coalescence, and surface roughness during the growth of polycrystalline films, *Journal of Applied Physics*, Vol. 90, Issue 10, 2001, pp. 5097-5103.
- [4]. N. B. Pilling, R. E. Bedworth, The Oxidation of Metals at High Temperatures, *J. Inst. Met.*, Vol. 29, Issue 1, 1923, pp. 529-591.
- [5]. Yu. Kuznetsov, A. Kolomeichenko, V. Goncharenko, I. Kravchenko, Investigation of Internal Stresses in Thin Layer Oxide Coatings on Aluminum Alloys, *Materials Science Forum*. Vol. 968, 2019, pp. 153-160.
- [6]. V. Shulgov, D. Shimanovich, V. Yakovtseva, G. Basov, Internal Stress in Aluminum Layers Deposited on Dielectric Substrates, in *Proceedings of the 3rd International Conference on Microelectronic Devices and Technologies (MicDAT'2020)*, 22-23 October 2020, pp. 51-52.
- [7]. J. D. Eshelby, The Continuum Theory of Dislocations in Crystals, in F. Seitz, Ed., *Solid State Physics*, Academic Press, New York, 1956, pp. 79-144.

